AIAA Guidance, Navigation, and Control Conference
13 - 16 August 2012, Minneapolis, Minnesota

AIAA 2012-4835

Adaptive Control for a VTOL UAV Operating Near a Wall

Daewon Lee*, Asad Ullah Awan†, Suseoung Kim‡and H. Jin Kim§
Seoul National University, Seoul, 151-742, Republic of Korea

In this paper, we proposed a neural-network-based adaptive controller to adapt against unknown, possibly time varying, external disturbances for a quadrotor UAV. The proposed algorithm can estimate uncertain forces, which occurs when flying in narrow areas, near walls and/or other surfaces, so that the controller can maintain satisfactory position tracking performance despite these disturbances. A proof for stability with the proposed algorithm is provided. Experimental results show that, with the proposed NN based adaptation algorithm, position tracking performance of quadrotor UAV shows satisfactory improvement in presence of external disturbances.

Nomenclature

F_i	Thrust force of the i-th rotor, [N]
f_{ex}	External disturbance vector.
m	Mass of the quadrotor, [kg]
J_x, J_y, J_z	Moment of inertia, [kg·m^2]
ρ	Force-to-moment scaling factor, [m]
g	Gravity, [m/s^2]
R_B^I	Coordinate transformation matrix from body frame to inertial frame
l	Length of the bar from the center of the quadrotor to each rotor, [m]
$\overrightarrow{e_z}$	Unit vector in the vertical upward direction in inertial coordinate frame
x, y, z	x, y, z position, [m]
ϕ, θ, ψ	Roll, pitch, yaw angle [rad]
u_1, u_2, u_3, u_4	Quadrotor control inputs for altitude, roll, pitch, and yaw.
$\mathbf{x}$	System state vector
μ_i	Center of the receptive field of the Gaussian kernel.
$\kappa(\dot{\mathbf{x}}, \mu_i)$	Gaussian radial basis kernel function.
$H(\dot{\mathbf{x}})$	Gaussian radial basis kernel function vector.
σ	Width of the Gaussian function
$\mathcal{L}$	Lyapunov function
S	Sliding surface in system control design
δ_z,δ_ϕ,δ_θ,δ_ψ	Uncertain force and moments
Δ	Uncertain term in the control system
N	Number of neurons in the neural networks system
ζ_i, λ	Weights, weighting vector for neural networks
C_1, C_2	Input gain matrix, Input gain vector.
γ	Update rate in adaptive control system

Subscripts and Superscripts

S	Slack variable

*Graduate Student, School of Mechanical and Aerospace Engineering: lee.daewon@gmail.com
†Graduate Student, School of Mechanical and Aerospace Engineering: asadawan01@gmail.com
‡Graduate Student, School of Mechanical and Aerospace Engineering: mer911tb@gmail.com
§Associate Professor, School of Mechanical and Aerospace Engineering: hjinkim@snu.ac.kr

r	Reference signal
$\hat{\cdot}$	Estimation value of variable $(\cdot)$
$\tilde{\cdot}$	Error between estimation and true value

I. Introduction

Quadrotor unmanned aerial vehicles (UAVs) are becoming increasingly popular among researchers around the world for implementing to turn their theory into practice. These vehicles offer the flight characteristics achievable with helicopters, namely stationary, vertical, longitudinal and lateral flight in a wide speed range, with a much simpler mechanical structure. With their small diameter and electrically driven rotors, these platforms are safer to operate than helicopters in indoor research environments. These advantages qualify these vehicles to be used in a variety of research applications.

Quadrotor UAVs exhibit highly-coupled nonlinear underactuated dynamics. This is further complicated by external disturbances and/or un-modeled dynamics, which make the task of autonomous flight control a challenging one. This has led to the development of various nonlinear and/or robust control techniques for the system. For example,[1] presents an internal-model-based error-feedback dynamic regulator that is robust to parametric uncertainty. Sliding mode disturbance observers[2] and adaptive-fuzzy control techniques[3] have also been used to make the system more robust to external disturbances. A combined controller and observer using neural networks is used in[4] to track reference trajectories. Robust control with nonlinear H-infinity techniques has been applied to uncertain parametric models.[13]

Many applications such as localization and mapping of the quadrotor UAV involve operation in indoor or tight space. In environments with limited space, such as a narrow corridor, significant external disturbances can affect the UAV. Operations involving very low altitude flight, such as picking up objects from the ground or landing, are also accompanied by a ground effect force. In a slow flight or stationary hover near the surface, it is known that the rotors generate downwash producing high-velocity outwash vortices to a distance approximately three times the diameter of the rotor. When rotor downwash hits the surface, if the resulting outwash vortices can affect the vehicle in all directions. In forward flight, departing or landing, high-speed trailing vortices are also produced. Other sources of disturbances such as wind gusts in outdoor environments can also adversely affect flight control. It is not tractable to accurately model these effects, especially in the form useful for control purposes.[15]

In one of our previous work,[6] precise position control of the quadrotor UAV has been considered for external disturbance forces which are stationary (i.e. zero time derivative). However, in practice, these disturbances forces can be time varying. Neural networks are a powerful tool for modeling unknown dynamics due to their universal function approximation property. In,[12] a NN-based strategy to adapt to the uncertain forces along the z-axis is considered and a stability is proved. As an extension of that work, in this paper, we present adaption rules for unknown time-varying forces along x, y and z-axes, along with experimental results.

This paper is organized as follows. Section 2 describes the quadrotor UAV dynamic model. Section 3 describes the development of an adaptive sliding mode controller for position tracking of the UAV. Section 4 presents the experimental setting and results for the proposed technique applied for our UAV platform. Conclusion and future directions are discussed in Section 5.

II. Quadrotor Helicopter Model

The quadrotor UAVs considered in this paper consist of four rotating fixed-pitch-angle blades as shown in Fig. 1, unlike classic helicopters that have variable-pitch-angle blades. The motion of the quadrotor helicopter is controlled by varying the speed of each rotor. The concept of operating the quadrotor helicopter is depicted in Fig. 1. Each individual rotor produces lift force and moment about the center of rotation. The two pairs of rotors, i.e. rotors 1 and 3, and rotors 2 and 4 in Fig. 1, rotate in opposite directions. To make a roll angle (ϕ) with respect to the x-axis of the body frame, the angular velocity of the rotor 2 can be increased and the angular velocity of the rotor 4 can be decreased while keeping the total thrust constant. Likewise, the angular velocity of the rotor 3 is increased and the angular velocity of the rotor 1 is decreased to produce a pitch angle (θ) with respect to the y-axis of the body frame. In order to perform yawing motion (ψ) with respect to the z-axis of the body frame, the speed of the rotors 1 and 3 are increased and the speed of the

rotors 2 and 4 are decreased. Motion along the z-axis is achieved by varying the cumulative thrust of all the four rotors.

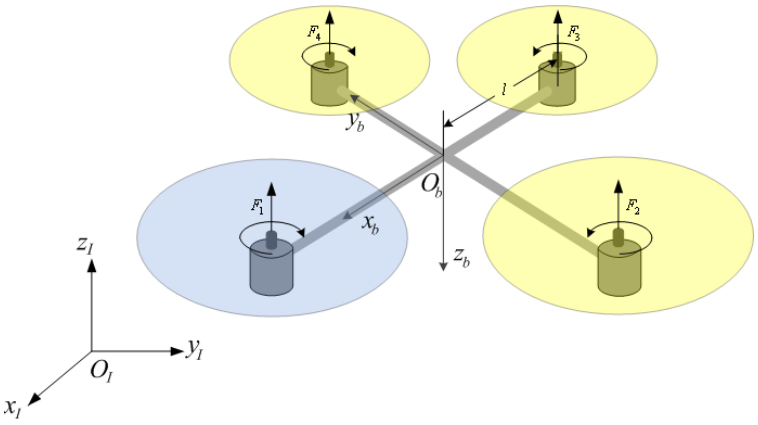

Figure 1. Configuration of the quadrotor helicopter

The equations of motion for the quadrotor without consideration of air drag can be presented as below.[5,6]

$$\begin{bmatrix} \ddot{x} \\ \ddot{y} \\ \ddot{z} \end{bmatrix} = \frac{1}{m}(\sum_{i=1}^{4} F_i) R_B^I \overrightarrow{e}_z + (\frac{F_{gr}(z)}{m} - g)\overrightarrow{e}_z \tag{1}$$

$$\begin{aligned} \ddot{\phi} &= l(F_2 - F_4)/J_1 \\ \ddot{\theta} &= l(-F_1 + F_3)/J_2. \\ \ddot{\psi} &= \rho(F_1 - F_2 + F_3 - F_4)/J_3 \end{aligned} \tag{2}$$

Here, $\overrightarrow{e}_z$ denotes the unit vector in the vertical direction in the inertial coordinate frame, $[x, y, z]$ denotes the position of the quadrotor in the inertial frame, and $[\phi, \theta, \psi]$ are roll, pitch, and yaw angles, respectively defined in the body frame. R_B^I represents the coordinate transformation matrix from body frame to inertial frame and g represents the acceleration due to gravity. Each rotor is located at a distance of l along the four cross bars from the center of gravity. J_i is the moment of inertia with respect to each axis and ρ is the force-to-moment scaling ratio. The quadrotor UAV is assumed to be symmetric with respect to the x and y axes so that the center of gravity is located at the center of the quadrotor. The physical control inputs to the motors are voltage signals v_i that are proportional to rotor angular velocity ω_i, and there is a one-to-one relationship between angular velocity and motor thrust F_i, which is determined experimentally.

$$F_i = K_{\omega i}\omega_i^2 \tag{3}$$

$$\omega_i^2 = h_i(v_i) \tag{4}$$

Therefore, for simplicity of expression and easier understanding, in place of motor input voltage v_i, we consider the inputs to the quadrotor system dynamics as the thrust forces, denoted as $F_1, \cdots, F_4$, acting perpendicular to the x-y plane as shown in Fig. 1.

In order to simplify Eqs. (1) and (2), input terms are defined as Eq. (5). u_1 is the control input of the total lift force, and u_2, u_3, and u_4 correspond to the control inputs of roll, pitch, and yaw moments, respectively.

$$\begin{aligned} u_1 &= (F_1 + F_2 + F_3 + F_4)/m \\ u_2 &= (F_2 - F_4)/J_x \\ u_3 &= (-F_1 + F_3)/J_y \\ u_4 &= \rho(F_1 - F_2 + F_3 - F_4)/J_z \end{aligned} \tag{5}$$

Then the equations of motion can be represented as Eq. (6)-(11)

$$\ddot{x} = u_1(\cos\phi\sin\theta\cos\psi + \sin\phi\sin\psi) \quad (6)$$
$$\ddot{y} = u_1(\cos\phi\sin\theta\sin\psi - \sin\phi\cos\psi) \quad (7)$$
$$\ddot{z} = u_1(\cos\phi\cos\theta) - g + \delta_z \quad (8)$$
$$\ddot{\phi} = u_2 l + \delta_\phi \quad (9)$$
$$\ddot{\theta} = u_3 l + \delta_\theta \quad (10)$$
$$\ddot{\psi} = u_4 + \delta_\psi \quad (11)$$

or, equivalently, using $\mathbf{x} = [x, y, z, \phi, \theta, \psi]^T$ and $\mathbf{u} = [u_1, u_2, u_3, u_4]^T$, in the vector form as Eq. (12).

$$\ddot{\mathbf{x}} = f(\mathbf{x}) + g(\mathbf{x})\mathbf{u} + f_{ex}(\mathbf{x}) \quad (12)$$

$$f(\mathbf{x}) = \begin{bmatrix} 0 \\ 0 \\ -g \\ 0 \\ 0 \\ 0 \end{bmatrix}$$

$$g(\mathbf{x}) = \begin{bmatrix} \cos\phi\sin\theta\cos\psi + \sin\phi\sin\psi & 0 & 0 & 0 \\ \cos\phi\sin\theta\sin\psi - \sin\phi\cos\psi & 0 & 0 & 0 \\ \cos\phi\cos\theta & 0 & 0 & 0 \\ 0 & l & 0 & 0 \\ 0 & 0 & l & 0 \\ 0 & 0 & 0 & 1 \end{bmatrix}$$

$$f_{ex}(\mathbf{x}) = \begin{bmatrix} 0 \\ 0 \\ \delta_z \\ \delta_\phi \\ \delta_\theta \\ \delta_\psi \end{bmatrix}$$

In Eq. (6)-(11), the additional terms $\delta_z, \delta_\phi, \delta_\theta$ and δ_ψ represent the unknown additional disturbances that arise due to situations described in Section I. A graphical illustration of 2 the disturbance δ_z caused by the so called ground effect that arises due to the interference of the downflow of air created by the rotors when flying close to the ground. Similiar situation arises when the UAV is flying close to the wall, causing disturbances represented by $\delta_\phi, \delta_\theta, \delta_\psi$.

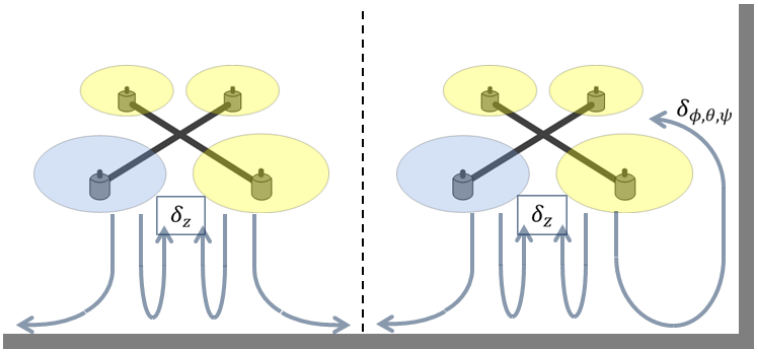

Figure 2. Illustration of disturbances arising from proximity to ground surfaces and walls

III. Adaptive Sliding Mode Controller for a Quadrotor Helicopter

In this section , we design an adaptive sliding mode controller for the quadrotor that guarantees asymptotic tracking of reference position under uncertain disturbances.

III.A. Adaptive Sliding Mode Control with Augmented Inputs

In order to design a sliding mode controller, we require the matrix $g(\mathbf{x})$ of Eq. (12) to be invertible. However, in this case $g(\mathbf{x})$ is a 6-by-4 matrix, which is not invertible. We tackle this problem by augmenting a 6-by-2 matrix $\mathbf{g}_s$ to $g(\mathbf{x})$ and slack variables $\mathbf{u}_s$ to $\mathbf{u}$ in order to form a square system. We can then rewrite the system dynamics of Eq. (12) as

$$\ddot{\mathbf{x}} = f(\mathbf{x}) + G(\mathbf{x})U - \nu + f_{ex}(\mathbf{x}) \,, \tag{13}$$

where $G = [g(\mathbf{x}),\ \mathbf{g}_s]$, $U = [\mathbf{u}^T,\ \mathbf{u}_s^T]^T$, and $\nu = \mathbf{g}_s\mathbf{u}_s$. $\mathbf{g}_s$ is set to be a constant matrix and defined in advance to make $G(\mathbf{x})$ invertible, whereas $\mathbf{u}_s = [u_5, u_6]^T$ are the slack variables. If we set

$$\mathbf{g}_s = \begin{bmatrix} 1 & 0 & 0 & 0 & 0 & 0 \\ 0 & 1 & 0 & 0 & 0 & 0 \end{bmatrix}^T \,, \tag{14}$$

then $\nu = \mathbf{g}_s\mathbf{u}_s = \begin{bmatrix} u_5 & u_6 & 0 & 0 & 0 & 0 \end{bmatrix}^T$. We are, therefore, required to estimate the slack variables u_5 and u_6.

Let $\mathbf{e} = \mathbf{x} - \mathbf{x}_r$ denote the error vector with respect to the vector of desired state variables $\mathbf{x}_r = [x_r, y_r, z_r, \phi_r, \theta_r, \psi_r]^T$, and define the sliding surface as

$$S = [s_1, s_2, s_3, s_4, s_5, s_6]^T = \dot{\mathbf{e}} + K\mathbf{e} \tag{15}$$

where $K = diag[k_1, \cdots, k_6]$ is a diagonal matrix with positive entries, so that the trajectory of the system could follow the desired references on the sliding surface $S = \mathbf{0}$.

The quadrotor UAV is an under-actuated system, i.e. the x and y state variables cannot be controlled directly from the control inputs. Let us define the references for $\dot{\phi}$ and $\dot{\theta}$ as Eqs. (16) and (17) to control the x and y positions.

$$\phi_r = (\dot{y} - \dot{y}_r) + k_\phi\,(y - y_r) \tag{16}$$

$$\theta_r = (\dot{x} - \dot{x}_r) + k_\theta\,(x - x_r) \tag{17}$$

where k_ϕ and k_θ are proportional gains.

In Eq. (13), we need to to cancel the nonlinear terms. We, therefore, need to define the estimated values of ν and $f_{ex}(\mathbf{x})$, which we denote as $\hat{\nu}$ and $\hat{f}_{ex}(\mathbf{x})$, respectively. From here onward, we use tilde ($\tilde{}$) to denote the difference between the true and estimated values, denoted by ($\hat{}$).
We can lump $-\nu$ and f_{ex} together into one uncertainty term defined as

$$\Delta = -\nu + f_{ex} = [u_5, u_6, \delta_z, \delta_\phi, \delta_\theta, \delta_\psi]^T \tag{18}$$

Then equation (13) becomes,

$$\ddot{\mathbf{x}} = f(\mathbf{x}) + G(\mathbf{x})U + \Delta \tag{19}$$

Multilayer neural networks guarantee that a nonlinear function can be approximated to any desired boundary, which is known as the universal approximation capability.[?] This function approximation property of NNs is exploited to represent the nonlinear term Δ as

$$\Delta = \sum_{i=1}^{N} \zeta_i \kappa(\dot{\mathbf{x}},\ \mu_i) + \varepsilon = \lambda^T H(\dot{\mathbf{x}}) + \varepsilon \tag{20}$$

where N is the number of neurons, ε is the approximation error, which is assumed to be bounded $|\varepsilon| \le \varepsilon_M$ and $\lambda = [\zeta_1\ \ \zeta_2\ \cdots\ \zeta_N]^T \in \mathcal{R}^{N\times 6}$ are weights that satisfy the following assumption. Assumption 1: There exists a constant vector of weights λ^{*T} that minimizes $|\varepsilon|$:

$$\lambda^* \triangleq \arg\min_{\lambda} \left[\sup |\Delta - \lambda^T H(\dot{\mathbf{x}})|\right] \tag{21}$$

where $H(\dot{\mathbf{x}}) = [\kappa(\dot{\mathbf{x}},\ \mu_1)\ \ \kappa(\dot{\mathbf{x}},\ \mu_2)\ \ \cdots\ \ \kappa(\dot{\mathbf{x}},\ \mu_N)]^T$. Here $\kappa(\dot{\mathbf{x}}, \mu_i)$ represents the NN basis function. In general, the uncertainty (Δ) may also be a function of $\ddot{x}$, in which case $\ddot{x}$ also would be fed into the neural network. However, this study does not aim to deal with general types of system parametric uncertainties, and results show that feeding only $\dot{x}$ into the NN shows satisfactory performance to handle the system uncertainities.

In this study, the Gaussian radial basis kernel function is used

$$\kappa(\dot{\mathbf{x}},\ \mu_i) = \exp\left(-\frac{(\dot{\mathbf{x}} - \mu_i)^T\ (\dot{\mathbf{x}} - \mu_i)}{\sigma^2}\right) \tag{22}$$

where μ_i is the center of the receptive field and σ is the width of the Gaussian function.

Lemma 1. *Consider the quadrotor system dynamics and sliding surface given by Eqs.* (13) *and* (15)*, respectively. Let the augmented input vector be given by Eq.* (23)*:*

$$U \quad = \quad G^{-1}(\mathbf{x})[-f(\mathbf{x}) - \hat{\lambda}^T H(\dot{\mathbf{x}}) + \ddot{\mathbf{x}}_r - C_1 S - C_2 sign(S)]\ . \tag{23}$$

where $C_1 = diag(c_1, c_2, c_3, c_4, c_5, c_6)$ is an input gain matrix with positive entries, and C_2 is a positive constant gain larger than ε_M.

We define the update rule for $\dot{\hat{\lambda}}$ as

$$\dot{\hat{\lambda}} = \gamma H(\dot{\mathbf{x}}) S^T \tag{24}$$

where γ is the update rate. Then, $\dot{\mathbf{x}}$ converges to $\dot{\mathbf{x}}_r$ asymptotically.

Proof. Let the Lyapunov function be

$$\mathcal{L} = \frac{1}{2} S^T S + \frac{1}{2\gamma} tr[\tilde{\lambda}^T \tilde{\lambda}] \tag{25}$$

$$\begin{aligned} \dot{\mathcal{L}} \quad &= \quad S^T \dot{S} + \frac{1}{\gamma} tr[\tilde{\lambda}^T \dot{\tilde{\lambda}}] \\ &= \quad S^T (f(\mathbf{x}) + G(\mathbf{x})U + \Delta - \ddot{\mathbf{x}}_r) + \frac{1}{\gamma} tr[\tilde{\lambda}^T \dot{\tilde{\lambda}}] \end{aligned} \tag{26}$$

By substituting the input U from Eq. (23), Eq. (26) becomes

$$\dot{\mathcal{L}} = -S^T (C_1 S + C_2 sign(S) - \varepsilon) - tr[\tilde{\lambda}^T (H(\dot{\mathbf{x}}) S^T - \frac{1}{\gamma} \dot{\hat{\lambda}})]$$

where $\varepsilon_M \leq C_2$. By updating $\dot{\hat{\lambda}}$ as shown in Eq. (24), and with positive entries in C_1, we can write Eq. (26) as

$$\dot{\mathcal{L}} = -S^T (C_1 S + C_2 sign(S) - \varepsilon) \leq 0\ , \tag{27}$$

Thus, the trajectory goes to the set $\{\mathbf{x} \in \mathbb{R}^n | S(t) = \mathbf{x}(t) - \mathbf{x}_r(t) = 0\}$, which means that $\mathbf{x}$ converges to $\mathbf{x}_r$.□

The above analysis only proves the boundedness of $\tilde{\lambda}$. Suppose enough time T_{ss} has elapsed to reach the steady state condition of $S(t) \equiv 0,\ \forall t > T_{ss}$, and $sign(0) = 0$. Then from Eqs. (19), (20), and (23), we obtain $0 \approx \tilde{\lambda}^T H(\dot{\mathbf{x}}_r) + \varepsilon$. Therefore, for small ε and nonzero $H(\dot{\mathbf{x}}_r)$, we may have very small $\tilde{\lambda}$.

In special cases of $\varepsilon = 0$, Lemma 2 verifies that the uncertain parameters converge to their true value under the adaptation rules derived from Lemma 1.

Lemma 2. *Consider the dynamics of the quadrotor system and its input shown in Eqs.* (13) *and* (23)*. The estimated slack variables, $\hat{\nu}$ and $\hat{f}_{ex}$, converge to their true value as the system goes to the steady state.*

Proof. Combining Eqs. (13) and (23), we have

$$\ddot{\mathbf{x}} = -(\nu - \hat{\nu}) + (f_{ex} - \hat{f}_{ex}) + \ddot{\mathbf{x}}_r - C_1 S \,. \tag{28}$$

and Eq. (28) can be rewritten as

$$\dot{S} + C_1 S = -(\nu - \hat{\nu}) + (f_{ex} - \hat{f}_{gr}) \,. \tag{29}$$

As proven in Lemma 1, the sliding surface S converges asymptotically to zero. This means that, at steady state, (29) yields

$$\begin{aligned} \nu - \hat{\nu} &= f_{ex} - \hat{f}_{ex} \\ i.e. \begin{bmatrix} u_5 - \hat{u}_5 \\ u_6 - \hat{u}_6 \\ 0 \\ 0 \\ 0 \\ 0 \end{bmatrix} &= \begin{bmatrix} 0 \\ 0 \\ \delta_z - \hat{\delta}_z \\ \delta_\phi - \hat{\delta}_\phi \\ \delta_\theta - \hat{\delta}_\theta \\ \delta_\psi - \hat{\delta}_\psi \end{bmatrix} . \end{aligned}$$

Thus, the estimations ($\hat{u}_5, \hat{u}_6, \hat{\delta}_z, \hat{\delta}_\phi, \hat{\delta}_\theta$ and $\hat{\delta}_\psi$) will converge to their true values in steady state. □

If we use the standard sliding mode control rather than performing the adaptation for the slack variable ν and the disturbance f_{ex} as in Eqs. (18), the uncertain terms u_5, u_6, and F_{gr} will be contained in $\dot{\mathcal{L}}$ of Eq. (27) as below:

$$\dot{\mathcal{L}}_{non-adaptive} = -S^T(C_1 S + C_2 sign(S) - \varepsilon) - S^T[\nu - f_{ex}] < 0$$

Thus, in the non-adaptive case, it would be necessary to use an input gain, C, large enough to compensate ν and f_{ex} to make $\dot{\mathcal{L}}_{non-adaptive} < 0$. Comparison of $\dot{\mathcal{L}}$ in the above equation and Eq. (27) suggests that the adaptive sliding mode controller requires smaller input magnitude, which is a clear advantage in terms of reduced chattering and power usage.

IV. Experimental Results

IV.A. Hardware Description

The experimental setting with the quadrotor and landing target is shown in 3. The distance from each motor rotational axis to the center l of the quadrotor is 25 cm, the mass of the entire UAV system m is 0.8 kilograms (including battery) and the height of the Vicon marker located on top of the rotors is 25 cm from the ground. After control calculation, the reference commands are sent to the quadrotor by a 2.4 GHz radio control (R/C) transmitter which is connected to the PC via an Endurance R/C PCTx USB dongle, as shown in Fig.4.

The quadrotor is equipped with an inertial measurement unit (IMU), which provides estimates of the Euler angles. A Vicon[14] system measures the position from which the translational velocities are calculated.

IV.B. Algorithm Validation

We designed single-layer neural-network system with 40 neurons to estimate the uncertain forces. The neural-networks based adaptive sliding mode controller is employed to improve performance in environments which produce large external disturbances, such as near ground surface or wall. In order to validate the algorithm, we first fly the quadrotor in an open environment away from the 'wall' (flight case 1) followed by a flight close to the 'wall' (flight case 2), as shown in Figure 3 to demonstrate the effect of external disturbances in flight control performance. Both these flights are performed using the non-adaptive controller. After this, we perform a flight close to the 'wall' using the adaptation rule introduced earlier (flight case 3). The reference trajectory of the quadrotor for all these flights is periodic up-and-down motion along the z-axis, with the x and y references fixed at zero for all duration.

Fig.5 shows position trajectories without adaptation rules, for the flight case 1 (away from wall). The dotted line represents references and the solid line is actual values. The norm of the trajectory errors along

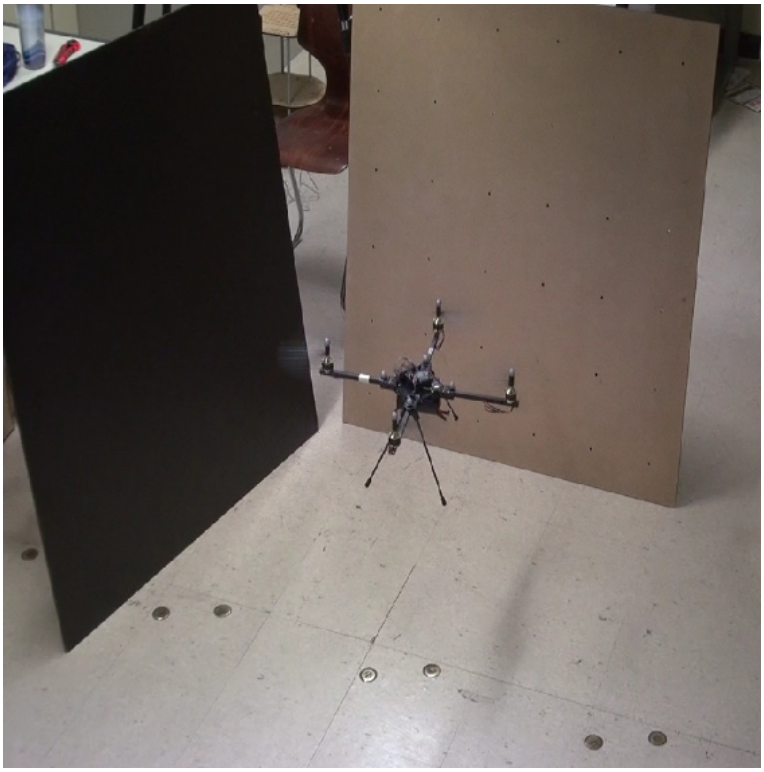

Figure 3. Experimental setup - quadrotor UAV flying close to the wall

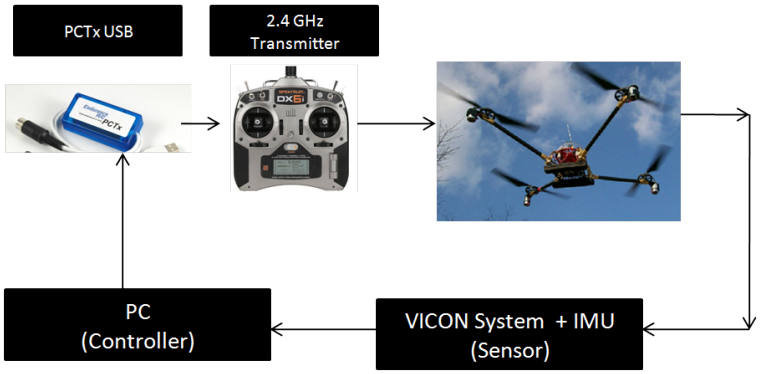

Figure 4. Block diagram of experimental setting

the x and y axes remain within 0.1 m. In the next flight (flight case 2), performed close to the wall again using the non-adaptive controller, however, the norm errors in x and y axes increase upto 0.2 m. This shows that the walls cause disturbances by reflecting the downwash of the quadrotor. Furthermore, results in the z axis show that the tracking performance is also adversely affected, so the both results require improvement.

Fig.7 shows results for position tracking for flight close to the wall using the proposed adaptation rule (flight case 3). Position tracking performances in x and y axes are not good as (flight case 1 - away from wall) due to the random nature of the turbulence, but there is a marked improvement over flight 2 due to the adaptation rule, especially along the z axis, hence proving the effectiveness of the proposed adaptation to external disturbances.

Fig.8 presents estimation values of uncertain forces Δ during the flight shown in Fig.7. When the quadrotor approaches the ground surface, where the ground effect force is significant (around 15s, 30s, 45s, 60s, 75s), Δ in z axis, $\hat{\delta}_z$, shows a corresponding increase.

To conform the performance of the proposed algorithm, so we repeat the flight set described above 12 times, and summerize the norm error during the flight for each axis as shown in Fig.9. Most flight results

show that the adaptive rules improve the control performances along the x and y directions.

A video of this experiment can be seen at $http://youtu.be/GPXAvs\_mYFE$.

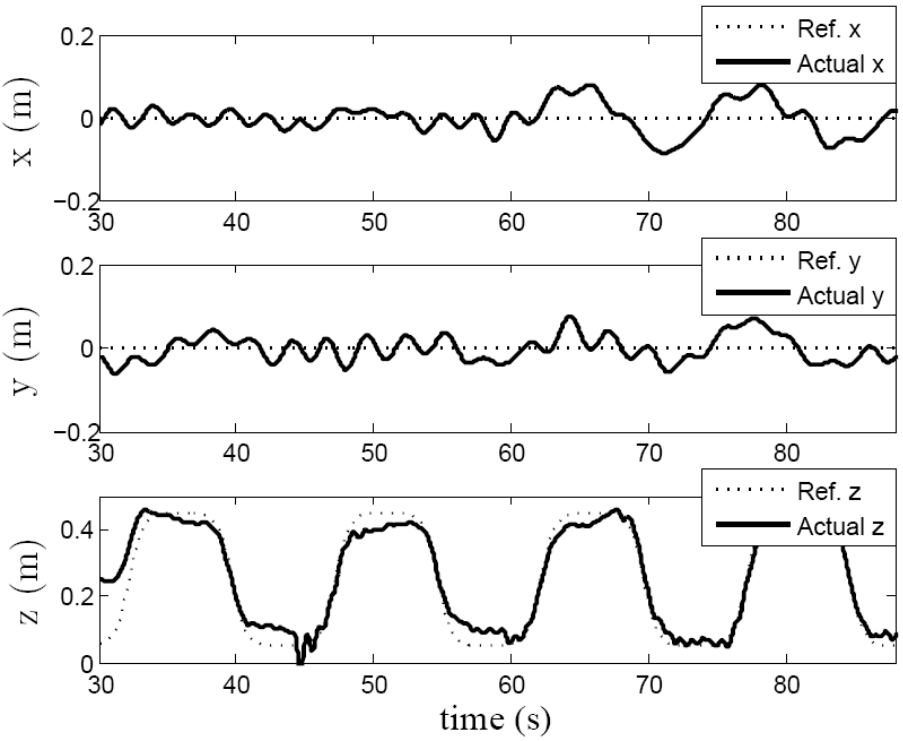

Figure 5. Position tracking results for flight case 1 - quadrotor flying in open environment away from wall, without adaptation

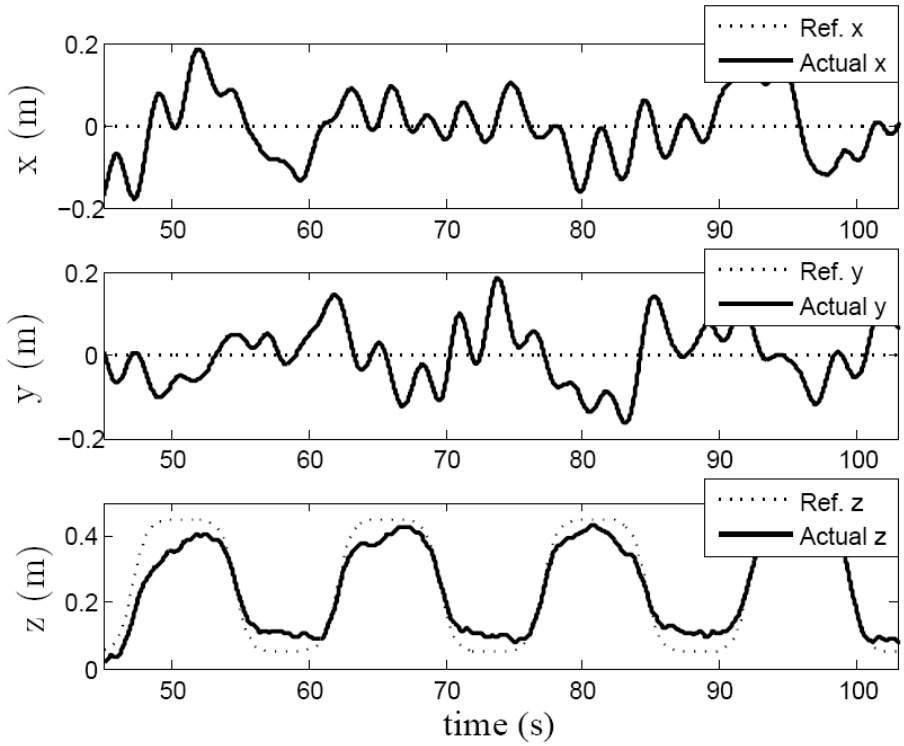

Figure 6. Position tracking results for flight case 2 - quadrotor flying close to wall, without adaptation

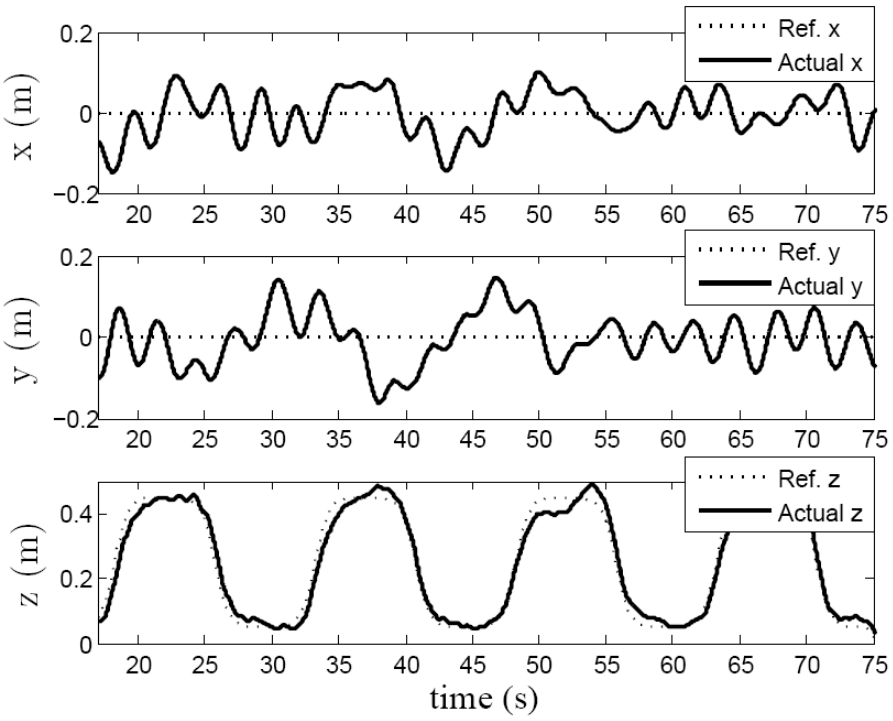

Figure 7. Position tracking results for flight case 3 - quadrotor flying close to wall, with proposed adaptation

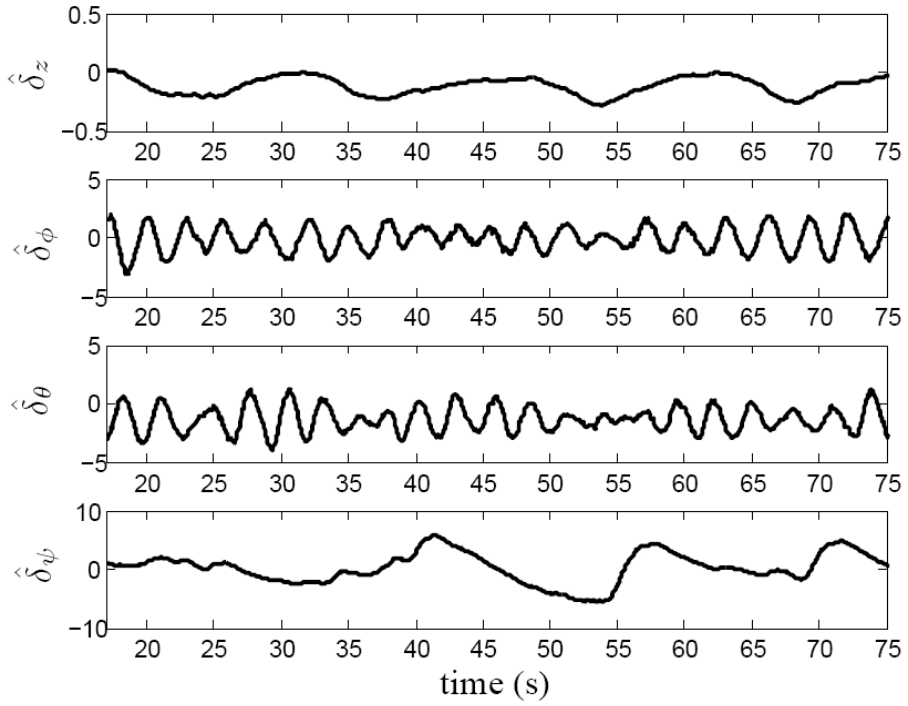

Figure 8. Plots showing disturbance forces estimated using the proposed algorithm during flight case 3

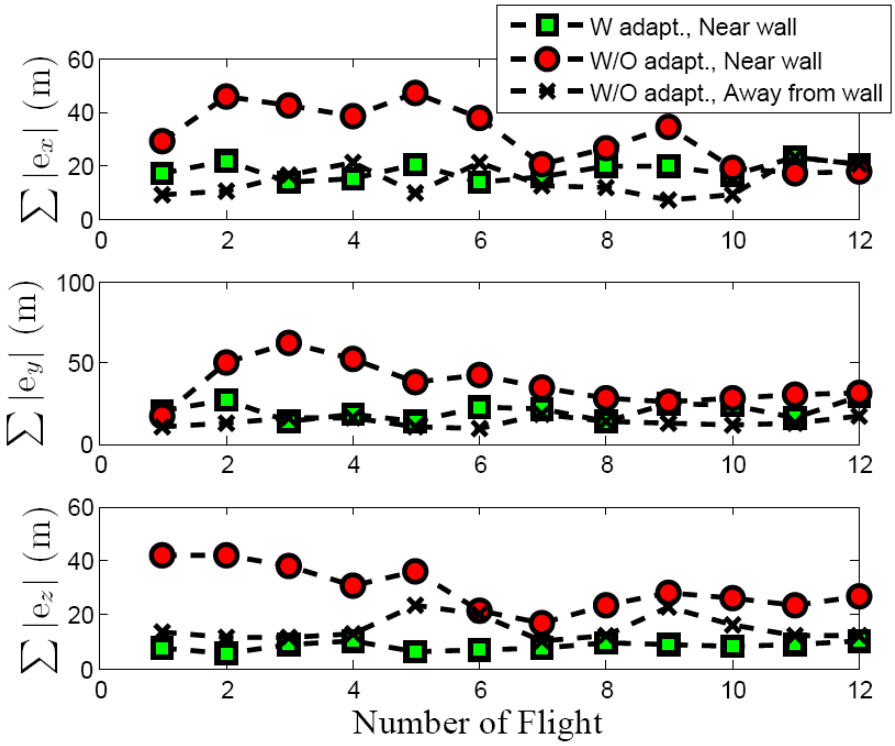

Figure 9. Plots showing the absolute error 1-norm in x,y and z axis for 12 different flights for all three flight cases i.e. without adaptation away from wall, without adaptation near wall and with adaptation near wall

V. Conclusion

In this paper, we proposed an adaptive controller based on a neural network to improve robustness against unknown, possibly time varying, external disturbances for a quadrotor UAV. The proposed algorithm can estimate uncertain forces acting on the quadrotor UAV, which are caused during flight in narrow areas, or near walls and surfaces. The stability of the overall control system with the proposed algorithm is proved. Experimental results show that, with the proposed NN-based adaptation algorithm, the quadrotor UAV shows satisfactory position tracking performance in the presence of external disturbances.

Acknowledgments

This work was supported by the National Research Foundation of Korea (NRF) grant funded by the Korea government (MEST) (No.2012-0000921) and KARI-University Partnership Program (Grant No. 2009-09-sunggwa-7) from the Korea Aerospace Research Institute (KARI).

References

[1] L. Marconi, A. Isidori, and A. Serrani, Autonomous vertical landing on an oscillating platform: An internal-model based approach, *Automatica, vol. 38, pp. 2132, 2002.*

[2] *L. Besnard, Y. Shtessel and B. Landrum, "Control of a Quadrotor Vehicle Using Sliding Mode Disturbance Observer,"* Proceedings of the 2007 American Control Conference*, pp. 5230-5235, 2007.*

[3] *C. Coza and C.J.B. Macnab, "A New Robust Adaptive-Fuzzy Control Method Applied to Quadrotor Helicopter Stabilization,"* NAFIPS 2006 Annual meeting of the North American Fuzzy Information Society*, pp. 454-458, 2006*

[4] *T. Dierks and S. Jagannathan, "Output Feedback Control of a Quadrotor UAV Using Neural Networks", IEEE Transactions on Neural Networks, Vol. 21, No. 1, 2010, pp. 50-66*

[5] *E. Altug, J. P. Ostrowski and R. Mahony, "Control of a quadrotor helocopter using visual feedback,"* Proceedings of the 2002 IEEE International Conference on Robotics and Automation*, pp. 72-77, 2002, Washington DC, Virginia, USA.*

[6] *D. Lee, H.J. Kim and S. Sastry, "Feedback linearization vs. adaptive sliding mode control for a quadrotor helicopter,"* International Journal of Control, Automation, and Systems*, Vol. 7, No. 3, pp. 419 - 428, 2009.*

[7] *D. Lee T. Ryan and H.J. Kim, "Autonomous Landing of a VTOL UAV on a Moving Platform Using Image-based Visual Servoing,"* IEEE International Conference on Robotics and Automation*, St. Paul, MN, USA, May 14-18, 2012.*

[8] *C. Pravitra, G. Chowdhary and E. Johnson, "A Compact Exploration Strategy for Indoor Flight Vehicles,"* IEEE Conference on Decision and Control and European Control Conference*, Orlando, FL, USA, 2011.*

[9] *S. Shen, N. Michael and V. Kumar "Autonomous Multi-Floor Indoor Navigation with a Computationally Constrained MAV,"* IEEE International Conference on Robotics and Automation*, Shanghai, China, 2011.*

[10] *M. Blosch, S. Weiss, D. Scaramuzza and R. Siegwart, "Vision Based MAV Navigation i nUnknown and Unstructured Environment,"* IEEE International Conference on Robotics and Automation*, Anchorage, AL, USA, 2010.*

[11] *S. Ahrens, D. Levine, G. Andrews and J. P. How, "Vision-Based Guidance and Control of a Hovering Vehicle in Unknown, GPS-denied Environments,"* IEEE International Conference on Robotics and Automation*, Kobe, Japan, 2009.*

[12] *D. Lee, H. Lim, H. J. Kim, Y. Kim, "Adaptive imagebased visual servoing for an under-actuated quadrotor system," AIAA Journal of Guidance, Control, and Dynamics, Vol. 35, No. 4, 2012.*

[13] *Raffo, G. Vianna, Ortega, M. G. Rubio, R. Franciso, "MPC with Nonlinear H-infinity Control for Path Tracking of a Quadrotor,"* Proc. of the 17th IFAC World Congress*, 2008*

[14] *www.vicon.com*

[15] *www.faa.gov/air_traffic/publications/atpubs/aim/Chap7/aim0703.html*